Technical Note

1967-20

A. G. Stanley

Electron Irradiation of P-Channel Junction FETs

13 April 1967

Prepared under Electronic Systems Division Contract AF 19(628)-5167 by

Lincoln Laboratory
MASSACHUSETTS INSTITUTE OF TECHNOLOGY
Lexington, Massachusetts

The work reported in this document was performed at Lincoln Laboratory, a center for research operated by Massachusetts Institute of Technology, with the support of the U.S. Air Force under Contract AF 19(628)-5167.

MASSACHUSETTS INSTITUTE OF TECHNOLOGY
LINCOLN LABORATORY

ELECTRON IRRADIATION OF P-CHANNEL JUNCTION FETS

A. G. STANLEY

Group 63

TECHNICAL NOTE 1967-20

13 APRIL 1967

LEXINGTON MASSACHUSETTS

ABSTRACT

The resistance of p-channel junction FETs to electron irradiation in high impedance nanoamp circuit applications is limited by the leakage current across the gate junction. The dependence of the leakage current on electron flux and total dose was investigated by electron irradiation in vacuum. The increase in leakage current was found to be primarily due to an increase in surface recombination velocity. It was independent of the electron flux over the range from 3×10^9 to 10^{12} $e/cm^2/sec$ with some indication of a reduction in leakage current at lower fluxes. An anomalously high leakage current due to channel formation developed in some devices at total doses above 10^{14} e/cm^2.

Accepted for the Air Force
Franklin C. Hudson
Chief, Lincoln Laboratory Office

ELECTRON IRRADIATION OF P-CHANNEL JUNCTION FETs

I. INTRODUCTION

P-channel junction FETs are more resistant to ionizing radiation than other active semiconductor devices. They are, therefore, exceptionally suitable for high impedance, low level circuits operating in a space radiation environment, limited only by radiation induced gate leakage currents (Ref. 1). In an earth sensor application leakage currents in the nanoampere range were sufficient to cause circuit failure. For this reason it became necessary to establish a radiation quality control check for these devices (Ref. 2). As a result a large number of the devices were irradiated under the conditions listed in Table I. It was noted that there were significant variations in the range of leakage currents developed under ostensibly the same conditions from one day to the next. This was all the more noticeable because the leakage currents of all the devices tested on a given day were well within one order of magnitude. The initial leakage currents always covered the same range, and there was no correlation between the leakage current before and after irradiation. Figure 1 shows some early results obtained on the 3 MeV Van de Graaff at Electronized Chemicals Corporation. A more detailed analysis of the leakage current distribution after irradiation to 5×10^{14} e/cm^2 is shown in Table II.

It was, therefore, decided to carry out a very careful study on all the parameters affecting the leakage currents of these devices after irradiation. The devices were irradiated in vacuum, since changes in humidity were considered to be one of the main causes of the observed fluctuations. Since the leakage current annealed fairly rapidly after irradiation at large electron fluxes, it was suspected that the leakage current produced by real time irradiation in space to the same total dose might be considerably smaller. A detailed study was, therefore, carried out on the flux dependence of the leakage current. This is believed to be the first study on the flux dependence of surface ionization effects in planar devices, except for work reported by Mitchell (Ref. 3) on Co^{60} irradiation of MOS capacitors.

TABLE I

Irradiation of P-Channel Junction FETs

Date	Facility	Run	Energy MeV	Electron Flux $e/cm^2/sec$	Total Dose e/cm^2	Bias Voltage	No. of Devices Tested	Remarks
6-10-65	E.C.C.		1.5	Varied	8.36×10^{14}	$V_{GS} = 15V$ $V_{DS} = -4.5V$	12	Including real time flux
7-6-65	"	1	1.5	5×10^{10}	3.78×10^{14}	"	12	"
		2	1.5	5×10^{10}	3.47×10^{14}	"	12	"
		3	1.5	5×10^{10}	5.39×10^{14}	"	12	"
7-8-65	"	1	1.5	5×10^{10}	3.8×10^{14}	"	12	"
		2	1.5	5×10^{10}	5.93×10^{14}	"	12	"
		3	1.5	5×10^{10}	4.17×10^{14}	"	12	"
7-9-65	"	1	1.5	5×10^{10}	3.48×10^{14}	"	12	"
		2	1.5	5×10^{10}	4.14×10^{14}	"	12	"
		3	1.5	5×10^{10}	3.48×10^{14}	"	12	"
9-27-65	"	1	1.5	5×10^{10}	4.1×10^{14}	"	12	
		2	1.5	5×10^{10}	4.2×10^{14}	"	12	
2-15-66	L.L. Air Scattering		1.0	4×10^{10}	4.5×10^{14}	$V_{GS} = 1.5V$ $V_{DS} = -6V$	98	"
4-20-66	"		1.0	5×10^{10}	4.5×10^{14}	"	70	
4-25-66	"		1.0	5×10^{10}	4.5×10^{14}	"	68	
5-18-66	"		1.0	5×10^{10}	5×10^{14}	"	99	
5-19-66	"		1.0	5×10^{10}	5×10^{14}	"	90	
5-20-66	"		1.0	5×10^{10}	5×10^{14}	"	15	Dummies and open cct devices
5-31-66	"		1.5	5×10^{10}	2×10^{14}	$V_{GS} = 1.5V$ $V_{DS} = -4.5V$	100	Real time annealing
6-1-66	"		1.0	Varied	7×10^{14}	"	100	"
6-2-66	"		1.0	5×10^{10}	2.3×10^{14}	"	100	"
8-17-66	L.L. Vacuum Chamber		1.0	1×10^{10}	6.9×10^{13}	"	1	pA measurements

TABLE I (Cont.)

Date	Facility	Run	Energy MeV	Electron Flux $e/cm^2/sec$	Total Dose e/cm^2	Bias Voltage	No. of Devices Tested	Remarks
9-23-66	L. L. Vacuum Chamber		1.5 and 1.0	1×10^{11}	1.26×10^{15}	$V_{GS} = 1.5V$ $V_{DS} = -4.5V$	5	
10-24-66	"		1.5	1×10^{11}	1×10^{15}	"	5	Temp. Variation
12-1-66	"		1.5	1×10^{10}	2.88×10^{14}	"	5	
12-2-66	"		1.5	1×10^{12}	1.08×10^{16}	"	5	
12-8-66	"		1.5	1×10^{9}	2.88×10^{13}	"	5	
12-13-66	"		1.5	3×10^{9}	8.1×10^{13}	"	5	
12-20-66	"		1.5	3×10^{8}	8.1×10^{12}	"	5	
12-28-66	"		1.5	1×10^{9}	2.7×10^{13}	"	5	Prestressed devices
12-29-66	"		1.5	1×10^{9}	2.7×10^{13}	"	5	

Table II - Gate-Leakage Current Distribution After Electron Irradiation to 5×10^{14} e/cm^2

Date	Total No. of Devices	Percentage Distribution																
		10^{-10} Amp. Range										10^{-9} Amp. Range						
		<1	1-2	2-3	3-4	4-5	5-6	6-7	7-8	8-9	9-10	1-2	2-3	3-4	4-5	5-6	6-7	7-8	>8
6-10-65	12			8.3	8.3	16.7	16.7	8.3	8.3		8.3	8.3	8.3						8.3
7-6-65*	36										5.5	83.2	5.5	2.8					2.8
7-8-65	12											58	42						
7-9-65**	12			8.3		8.3	8.3		16.3	8.3	8.3	41.8							
9-27-65**	24	4.2	33.3	16.7	16.7	8.3	12.5	4.2				4.2							
2-15-66	98	2.0		3.0	6.1	9.2	8.2	14.3	12.2	6.1	6.1	21.4	5.1	2.0	1.0	1.0		1.0	1.0
4-20-66	70			1.4	1.4	1.4	2.8	1.4		5.7	2.8	20.0	11.4	5.7	21.4	18.5	4.3		1.4
4-25-66	68		8.8	11.8	1.5	2.9	4.4	4.4	4.4	7.4	11.8	26.5	8.8	5.9	1.5				1.5
5-18-66	99		1.0	4.0	7.0	8.0	4.0	5.0	2.0	6.0	3.0	46.0	13.0						1.0
5-19-66	90											24.4	38.9	30	6.7				
10-24-66***	5												60	20					20
12-2-66***	5											20	60	20					

* includes unknown amount of background noise from facility
**4×10^{14} e/cm^2
***in vacuum

2. EXPERIMENTAL ARRANGEMENT

All the devices were taken from the same batch so as to ensure uniformity of fabrication. Five fresh units were used for each experiment. The TO18 cans of the FETs were inserted into tight fitting countersunk holes on a 3/16 in. copper plate which shielded the underside of the transistor and leads from scattered electrons (see Fig. 2). The copper plate was mounted inside the end dome of the 48 in. vacuum chamber of the Lincoln Accelerator Laboratory (Ref. 4). The temperature of the copper plate was kept constant to within $\pm$ 0.5°C by means of the temperature control system shown in Fig. 3. Water from a constant temperature bath was circulated through the copper plate. The bath temperature was controlled by means of a chilled water heat exchanger and a 500W heater. The latter was operated by an on-off temperature controller activated by a thermistor clamped to the underside of the copper plate. During most of the experiments the temperature was set at 25°C.

The terminals of the transistor sockets were connected by polyimide coated wires to specially constructed low leakage octal feed thrus. All wires connected to a given octal were kept at the same voltage as the gate, which in the FETs under test is internally connected to the body of the silicon chip and therefore to the header. This necessitated the test circuit shown in Fig. 4. The devices were kept under bias throughout the experiment. The bias voltages were selected in accordance with the application requirements.

The octal feed thrus were connected to the measuring circuit by means of 40 feet of wire with fiberglass insulation. The experiments were carried out under low humidity conditions in the facility which reduced the system d.c. leakage current to 20 pA. A.C. pickup was removed by means of 0.1 μF bypass capacitors. All experiments were run with a dummy transistor to measure background noise. The dummy consisted of a TO18 header and can from which the silicon chip had been removed.

During most of the experiments the devices were irradiated with 1.5 MeV electrons from the Lincoln Laboratory Van de Graaff. The electron flux was varied from 3×10^8 e/cm^2 to 1×10^{12} e/cm^2. The electron beam was

continuously monitored on a Faraday cup placed within 2 in. from the transistor under test and connected to a current integrator. The beam was uniform over an area of more than 6 in. diameter and could be observed on a fluorescent screen by means of closed circuit television. The devices were irradiated continuously to avoid annealing effects. Readings with the beam off were taken at 30 minute intervals and required less than 1 minute off time.

3. EXPERIMENTAL RESULTS

A. Total Dose and Electron Flux

Fig. 5 shows the gate leakage current vs. total electron dose as a function of electron flux. The results, which were obtained in a series of experiments over a period of three months, indicate the absolute reproducibility obtainable in a vacuum environment. The leakage current is unchanged up to a total dose of 10^{13} e/cm^2. Between 10^{13} and 10^{14} e/cm^2 it increases linearly and thereafter more slowly reaching saturation at about 7×10^{15} e/cm^2. The percentage spread in values is greatest from 10^{13} to 5×10^{14} e/cm^2.

The leakage current is independent of electron flux over the range from 3×10^9 to 10^{12} e/cm^2/sec. A maximum continuous machine time of 10 hours imposed a limit on the maximum total dose that could be attained at the lower electron fluxes. As a result a total dose of only 2.7×10^{13} e/cm^2 was reached at a flux of 10^9 e/cm^2/sec. At this dose some of the devices remained unchanged while others increased their leakage current in conformity with the values obtained at a flux of 3×10^9 e/cm^2/sec. At still lower fluxes the maximum total dose was insufficient to change the leakage current. The first two measurements carried out at a flux of 10^{11} e/cm^2/sec show lower readings than the rest of the curve. It appears that over the most steeply increasing part of the curve the leakage current is independent of the flux only after 1 hour of continuous irradiation.

Comparison with the earlier results obtained by irradiation in air (Fig. 1 and Table 2) indicates a slight increase in the mean leakage current

in vacuum. This seems to be due to changes in fabrication, since the vacuum measurements are in good agreement with the results obtained in air on the same batch of devices. The variance in the values obtained at a total dose of 5×10^{14} e/cm^2 has been very much reduced in the vacuum irradiation.

B. Effect of Electron Beam

All the measurements described above were made with the beam off. Under an electron flux of φ e/cm^2/sec an additional gate current of $\sim 7.5 \times 10^{-20}$ φ amps was produced which obscured the leakage current particularly at high fluxes. This is shown in Fig. 6 for fluxes of 10^{10} and 10^{11} e/cm^2/sec. The on readings exhibited considerable fluctuations caused by changes in the beam intensity. Under real time irradiation in space the electron induced current is insignificant.

The electron beam also produced a negative system leakage current of $\sim 1.5 \times 10^{-21}$ φ amps. All other currents measured in the circuit of Fig. 4 were positive.

C. Anomalous Leakage Current

The primary purpose of a radiation quality control check is to eliminate devices rendered defective by irradiation. Table III shows that in the FETs under test an anomalously high leakage current developed in some of the devices at total doses above 10^{14} e/cm^2. The onset of this condition is very sudden as shown in Fig. 7. A certain minimum period of time under irradiation must elapse before the onset of this phenomenon. Hence the total dose was lower at a flux of 10^{11} e/cm^2/sec than at a flux of 10^{12} e/cm^2/sec. No anomalous leakage currents were observed at still lower fluxes. It is therefore concluded that none would develop in a space environment.

D. Temperature Dependence

In one of the experiments the temperature under irradiation was varied over the range from 20 to 30°C at a total dose of 10^{15} e/cm^2. The temperature coefficients shown in Table IV amount to a change of only 4 - 7 per cent per °C for normal devices and to an even smaller change in the anomalous leakage current. All the temperature coefficients are positive.

TABLE III

Irradiation Induced Anomalous Leakage Current

Device	Flux	Onset of Anomalous Leakage Current		Maximum Leakage Current
		Total Dose	Time	
	$e/cm^2/sec$	e/cm^2	Minutes	amps
724	1×10^{12}	3.6×10^{15}	60	1.3×10^{-6}
725	1×10^{12}	9.6×10^{15}	160	1.1×10^{-7}
726	1×10^{12}	7.2×10^{15}	120	1.3×10^{-8}
714	1×10^{11}	1.8×10^{14}	30	3.9×10^{-7}
712	1×10^{11}	7.2×10^{14}	120	1.8×10^{-7}

TABLE IV

Temperature Dependence of Source-Gate Leakage Current

Total Dose: 10^{15} e/cm^2 Flux: 10^{11} e/cm^2/sec Beam Off Measurements

Device	Type	Leakage Current (Amps) 25.35°C T_o	20.6°C T_1	30.1°C T_2	Temp. Coefficient (Amps/°C) $\Delta I_R/\Delta T$ $T_o - T_1$	$T_2 - T_o$	Percentage Change in Temp/°C $\frac{100}{I_R} \cdot \frac{\Delta I_R}{\Delta T}$ $T_o - T_1$	$T_2 - T_o$
713	Normal	4.1×10^{-9}	3.0×10^{-9}	5.1×10^{-9}	2.3×10^{-10}	2.1×10^{-10}	6.5	4.7
715		6.8×10^{-9}	4.9×10^{-9}	8.6×10^{-9}	4.0×10^{-10}	3.8×10^{-10}	6.8	4.9
716		4.0×10^{-9}	3.0×10^{-9}	4.9×10^{-9}	2.1×10^{-10}	2.0×10^{-10}	5.9	4.4
712	Anomalous	1.6×10^{-7}	1.4×10^{-7}	1.9×10^{-7}	5.0×10^{-9}	5.4×10^{-9}	3.3	3.1
714		3.2×10^{-7}	2.7×10^{-7}	3.8×10^{-7}	1.1×10^{-8}	1.3×10^{-8}	3.6	3.6

E. Annealing

In a number of experiments an attempt was made to simulate real time irradiation by preirradiating the devices at a flux of 5×10^{10} e/cm^2/sec to a total dose of about 10^{14} e/cm^2 and then anneal out the leakage current under real time conditions, i.e. at a flux of 10^8 e/cm^2/sec under bias. The attempt failed on account of the time constants involved. Fig. 8 shows that very rapid annealing takes place for the first hour which is followed by very slow annealing with a time constant of days. Furthermore, exactly the same annealing pattern occurred in the absence of the electron irradiation.

F. Effect of Electron Energy

Variation of the electron energy from 1 to 1.5 MeV had no effect on the leakage current. This is to be expected since the stopping power in silicon (Ref. 5) and silicon dioxide (Ref. 6) are constant over this range.

G. Effect of Voltage Prestress

Some devices were kept under bias for one week before irradiation. This lowered the preirradiation leakage current by about 10 per cent but had no effect on the radiation induced leakage current.

H. Current-Voltage Characteristics

The current across the junction was measured as a function of applied voltage both in the reverse and forward direction by shorting source to drain and applying a voltage at the gate contact. The results are shown in Figs. 9 and 10.

Before irradiation the reverse current between 0.5 and 1V and again between 2 and 12V is proportional to the square root of the voltage. After irradiation the I-V characteristics of normal devices are very flat showing a typical voltage saturation curve brought about by saturation effects. In irradiated devices with anomalously high leakage currents there is a rapid rise in reverse current with voltage indicating avalanche breakdown.

The I-V characteristics were also measured in the forward direction in order to determine the nature of the current following the method described by Goben and Smits (Refs. 7, 8). The current I is proportional to $\exp(qV/nkT)$ where n varies over different current ranges depending on the mechanism involved (see Table V). Only the low current ranges have significance for the reverse leakage current. Brucker et al. (Ref. 9) have shown that for electron irradiation values of n between 1 and 2 are due both to recombination of minority carriers in the bulk depletion region and to an increase in the surface-recombination velocity. The bulk recombination takes place at defects located on the more lightly doped gate side of the depletion region. The increased surface recombination velocity may be due to the introduction of new interface states and also due to changes in surface potential leading to an increased recombination rate at the interface states already present. n values greater than 2 are due to the formation of surface channels (Ref. 10).

TABLE V

Interpretation of Forward I-V Characteristics

Current Type	Total Dose e/cm^2	Current Range Amps	n
	0	10^{-11} - 10^{-6}	1.3
Normal	1.8×10^{15}	5×10^{-10} - 10^{-7}	1.75
		10^{-6} - 10^{-4}	1.35
Anomalous	1×10^{16}	10^{-8} - 10^{-7}	2.25
		10^{-6} - 10^{-4}	1.5

4. COMPARISON WITH THEORY

An idealized structure of a planar p-channel junction FET is shown in Fig. 11. The gate leakage current is the current across the reverse biased p-n junctions from the n type gate and body regions to the p region extending

from the source through the channel to the gate. The n type body is connected internally to the gate.

The reverse characteristics of irradiated silicon junction diodes were first described by Xavier (Ref. 11). The leakage current I measured during irradiation may be expressed as the sum of 4 components:

$$I = I_R + I_P + I_{LR} + I_{LP} \tag{1}$$

where

I_R is the diode reverse leakage current in the absence of radiation;

I_P is the additional diode leakage current produced by the radiation;

I_{LR} is the system leakage current in parallel with the p-n junction in the absence of radiation. It includes the leakage across the terminals of the transistor header.

I_{LP} is the additional system leakage current produced by the radiation.

A. Leakage Current in the Absence of Radiation

The diode leakage current I_R is again the sum of three components:

$$I_R = I_d + I_{rg} + I_s \tag{2}$$

The diffusion component, I_d, also known as the reverse saturation current, is given by (Ref. 12).

$$I_d = q\,A n_i^2 \left(\frac{1}{N_A} \sqrt{\frac{D_n}{\tau_n}} + \frac{1}{N_D} \sqrt{\frac{D_p}{\tau_p}} \right) \tag{3}$$

where

N_A = acceptor concentration in p region

N_D = donor concentration in n region

D_n = electron diffusion constant in p region

D_p = hole diffusion constant in n region

n_i = intrinsic carrier concentration in silicon

τ_n = electron lifetime in p region

τ_p = hole lifetime in n region

A = junction area

q = electronic charge

The depletion layer recombination generation component I_{rg} at large reverse bias is given by (Ref. 13)

$$I_{rg} = q A n_i W / 2 \sqrt{\tau_n \tau_p} \tag{4}$$

The depletion layer width

$$W = \left[\frac{2 \epsilon_{si} (V_d + V_a)}{q} \left(\frac{1}{N_a} + \frac{1}{N_d} \right) \right]^{1/2} \tag{5}$$

where

V_a = applied voltage

V_d = difference in electrostatic potential between the n and p regions

ϵ_{si} = dielectric constant of silicon

The character and magnitude of the surface leakage component I_s depends on the formation of an inversion layer. In the structure under discussion an n-type inversion layer could form in the p^+ region of source and drain, but is to some extent inhibited by the heavy p doping in this region. In the absence of an inversion layer the surface leakage component is entirely due to electron-hole recombination at the surface of the depletion region and may be expressed in the form (Ref. 10, 14):

$$I_s = q n_i S W L_s \tag{6}$$

where S is the surface recombination velocity and L_s the junction perimeter.

The presence of an inversion layer gives rise to a channel current, i.e. an excess reverse current which saturates with increasing reverse bias. The inversion layer extends the effective junction area, thus producing the following additional leakage terms (Refs. 15, 16):

1. Recombination-generation current in the depletion region of the junction between the inversion layer and the substrate.

2. Recombination-generation current at the surface of the extended depletion region.

3. Current due to breakdown of the junction between the inversion layer and the underlying p^+ region. The breakdown proceeds through tunneling if the surface of the p^+ region is heavily doped and by an avalanche mechanism if it is lightly doped.

4. An ohmic current flows if the inversion region extends to the metallized source or drain.

Before irradiation I_R is about 5×10^{-11}A at 6V bias and consists primarily of a combination of the recombination-generation current I_{rq} and the surface component I_s as shown by the square root dependenc on the voltage. From Eqs. (4), (5) and (6)

$$I_R \simeq qn_i \left(\frac{A}{2\sqrt{\tau_n \tau_p}} + SL_s \right) \left[\frac{2\varepsilon_{si}(V_d + V_a)}{q} \left(\frac{1}{N_a} + \frac{1}{N_d} \right) \right]^{1/2} \quad (11)$$

The system leakage current I_{LR} during the experiment was 2×10^{-11} A.

B. Electron Beam Induced Current

The additional diode leakage current I_P during irradiation also has diffusion, recombination-generation and surface components:

$$I_P = I_{dP} + I_{rgP} + I_{sP} \quad (7)$$

The electron flux generates G hole-electron pairs per unit volume in the silicon which is given by

$$G = -\frac{dE}{dx}\,\frac{\varphi}{e_n} \tag{8}$$

where $-\frac{dE}{dx}$ is the stopping power in silicon in ev/cm

φ is the electron flux in $e/cm^2/sec$

e_n is the energy required to generate one hole-electron pair
= 4.2 eV for silicon (Ref. 17)

Then (Ref. 11)

$$I_{dP} = qGA\,(\sqrt{D_n\tau_n} + \sqrt{D_p\tau_p}) \tag{9}$$

$$I_{rgP} = q\,GAW \tag{10}$$

I_{sP} is rather complex if an inversion layer is formed, but is always proportional to the flux. All three components I_{dP}, I_{rgP} and I_{sP} make significant contributions to the electron beam induced current.

C. Radiation Damage

All current components are affected by radiation damage through decrease in the lifetimes, increase in surface recombination velocity and formation of inversion layers. By making measurements only with the electron beam off the number of relevant components is reduced to the recombination-generation component I_{rg} and the surface component I_s.

I_{rg} depends on the lifetimes τ_n and τ_p which are reduced by the introduction of bulk defects:

$$\frac{1}{\tau} = \frac{1}{\tau_o} + K\Phi \tag{12}$$

where τ_o is the initial lifetime, Φ the total electron dose and K a damage constant. The recombination-generation current after irradiation is therefore a function of the total dose:

$$(I_{rg})_{irrad} = I_{rgo}(1 + \tau_o K \Phi) \quad (13)$$

The surface component I_s depends on the surface recombination velocity S and on the formation of inversion layers. Fitzgerald and Grove (Ref. 18) have shown that S may increase from 5 to 1000 cm/sec by irradiation with moderate doses of X-rays. I_s is usually a non-linear function of Φ and levels off after saturation of the surface traps. Inversion layers produce a large increase in I_s by many orders of magnitude.

The interpretation of the I_p vs. Φ curve shown in Fig. 5 is ambiguous. There is an approximately linear range from 10^{13} to 10^{14} e/cm^2 followed by a square root dependence and ultimate saturation at 10^{16} e/cm^2. The latter suggests a predominance of the surface component.

D. Temperature Dependence

The temperature dependence of I_{rg} is determined by the intrinsic carrier concentration

$$n_i \sim T^{3/2} \exp(-E_G/2kT) \quad (14)$$

where E_G, the band gap for silicon, is 1.21 eV.

Then
$$\frac{dI}{dT} = \frac{I}{T^{1/2}}\left(\frac{E_g}{2kT} + \frac{3}{2}\right) \quad (15)$$

$$\sim 1.4\ I \text{ at } 25^{\circ}C$$

Table IV shows that the temperature coefficient after radiation is more than one order of magnitude smaller than this. The small positive temperature coefficient observed is in agreement with the model of Grove and Fitzgerald (Ref. 16), i.e. a breakdown of the junction between an inversion layer and the underlying p^+ region by means of an avalanche mechanism.

5. CONCLUSIONS

The increase in the gate leakage current with electron irradiation is primarily due to an increase in the surface recombination velocity. This is shown by saturation of the current on increasing either the inverse voltage or the total electron dose and by the small positive temperature coefficient. It is also in agreement with the forward I-V characteristics at low current levels and with the very slow annealing behavior at ambient temperatures. An anomalously high leakage current formed in some devices at total electron doses above 10^{14} e/cm^2 is due to channel formation in the p region resulting in avalanche breakdown.

The gate leakage current was found to be independent of electron flux over the range from 3×10^9 to 10^{12} e/cm^2/sec for continuous exposures up to 10 hours. Some indication was found that more prolonged irradiation at still lower fluxes may result in a lower leakage current at a fixed total dose. This is also supported by annealing time constants of the order of days at ambient temperatures.

The above represents a fundamental problem in the simulation of space radiation effects resulting in surface ionization phenomena with long time constants. In order to study such phenomena it is necessary to expose the devices under bias to sources of ionizing radiation continuously for periods of weeks or months. Sr^{90} is the optimum source for this purpose, as it approximates the electron spectrum in the outer Van Allen belt and is uncontaminated by gamma emission. An extension of the experiments using such a source is being planned.

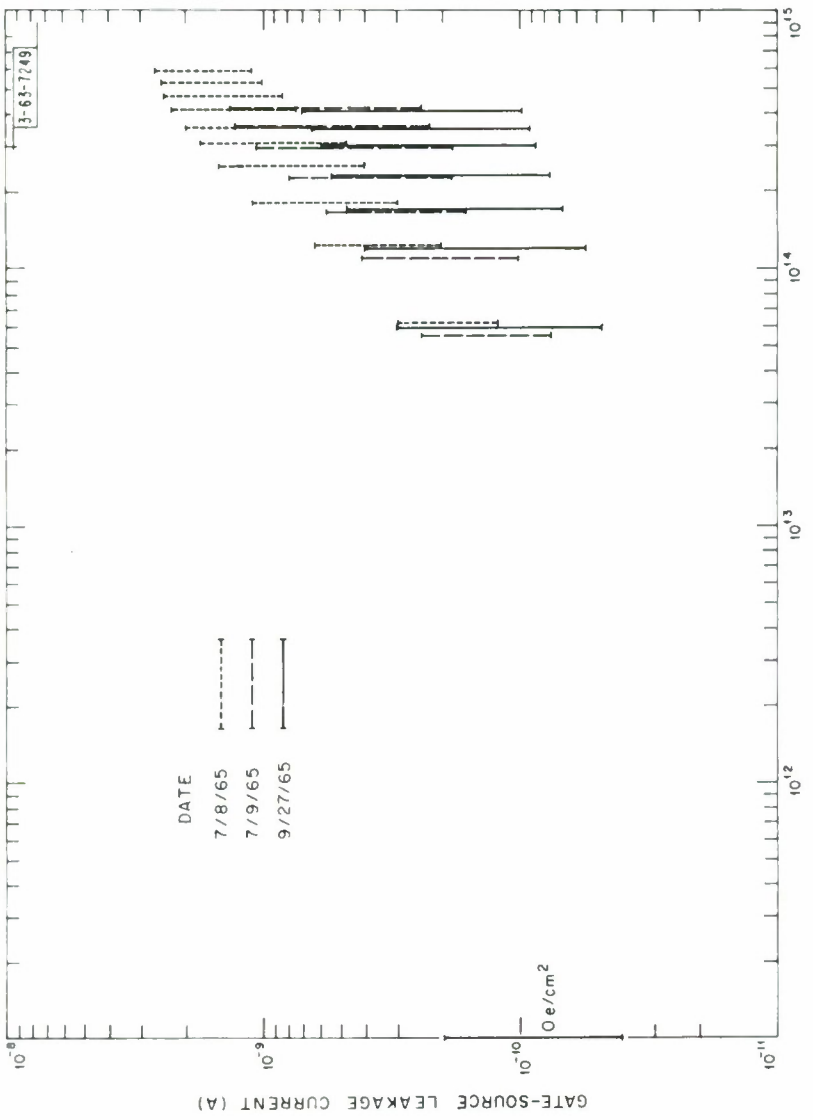

Fig. 1. Gate-source leakage current vs. total dose
1.5 MeV electrons
5×10^{10} e/cm^2/sec

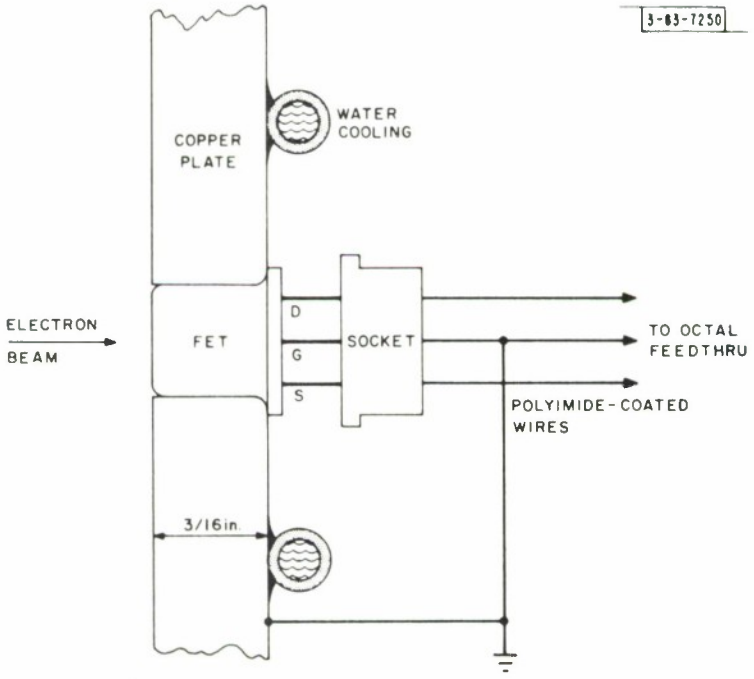

Fig. 2. Transistor mount.

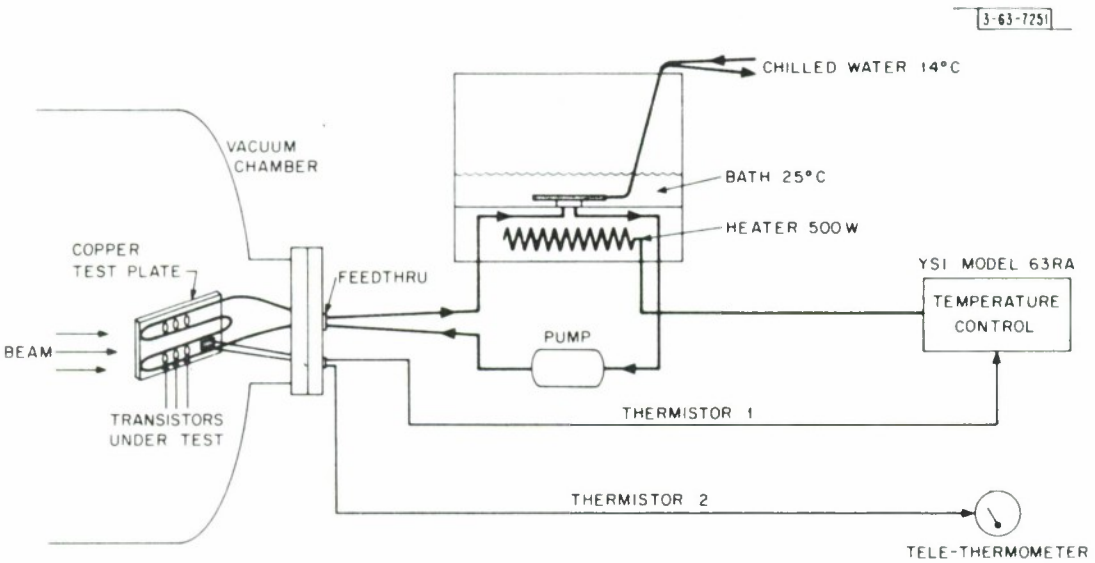

Fig. 3. Constant temperature system.

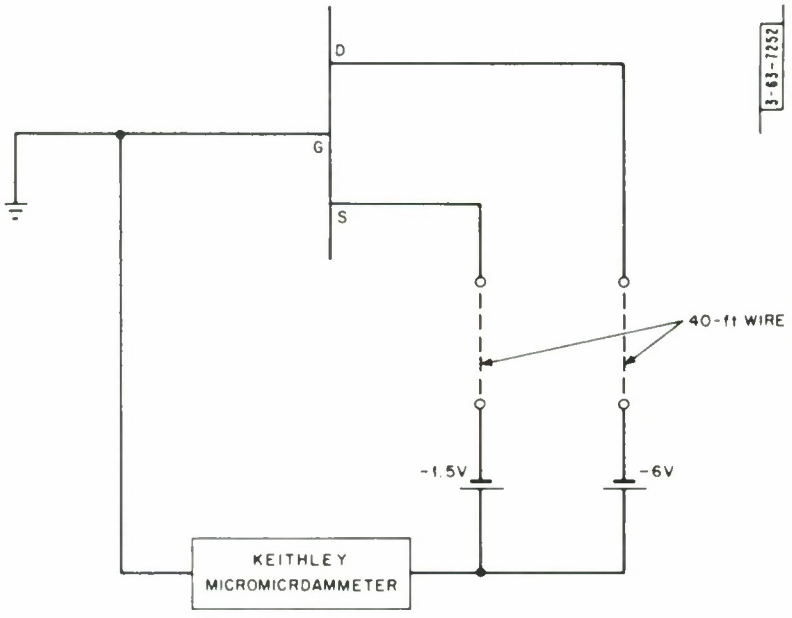

Fig. 4. Test circuit.

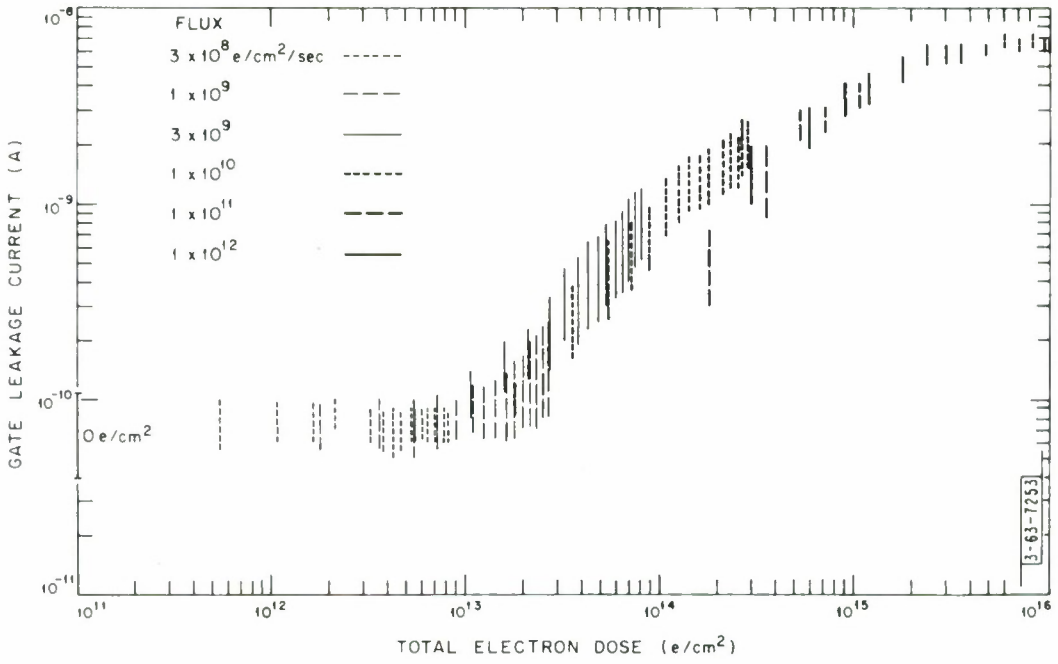

Fig. 5. Gate leakage current vs. total electron dose as function of electron flux

Beam off measurements, including system leakage current 2×10^{-11} A

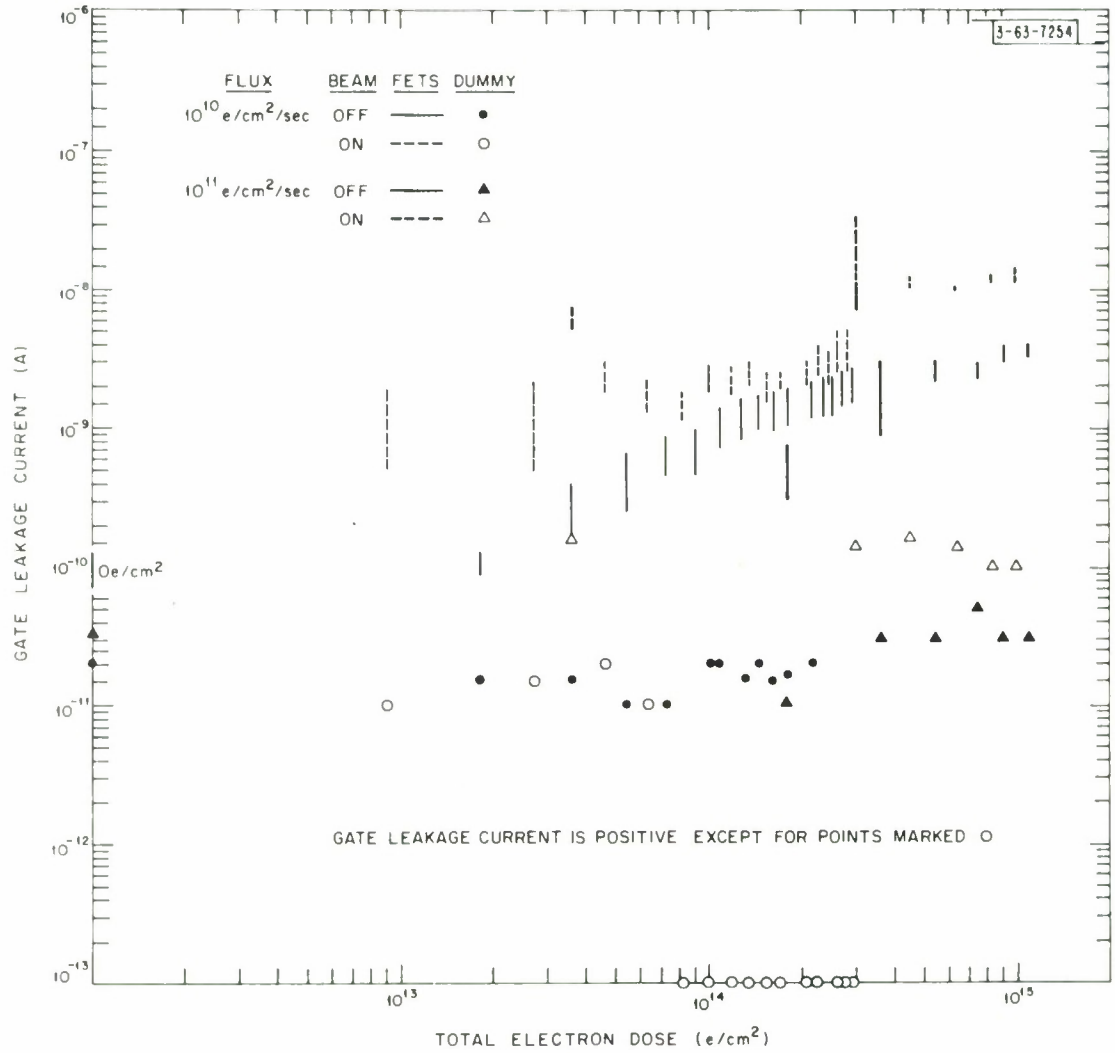

Fig. 6. Effect of electron beam on gate leakage current.

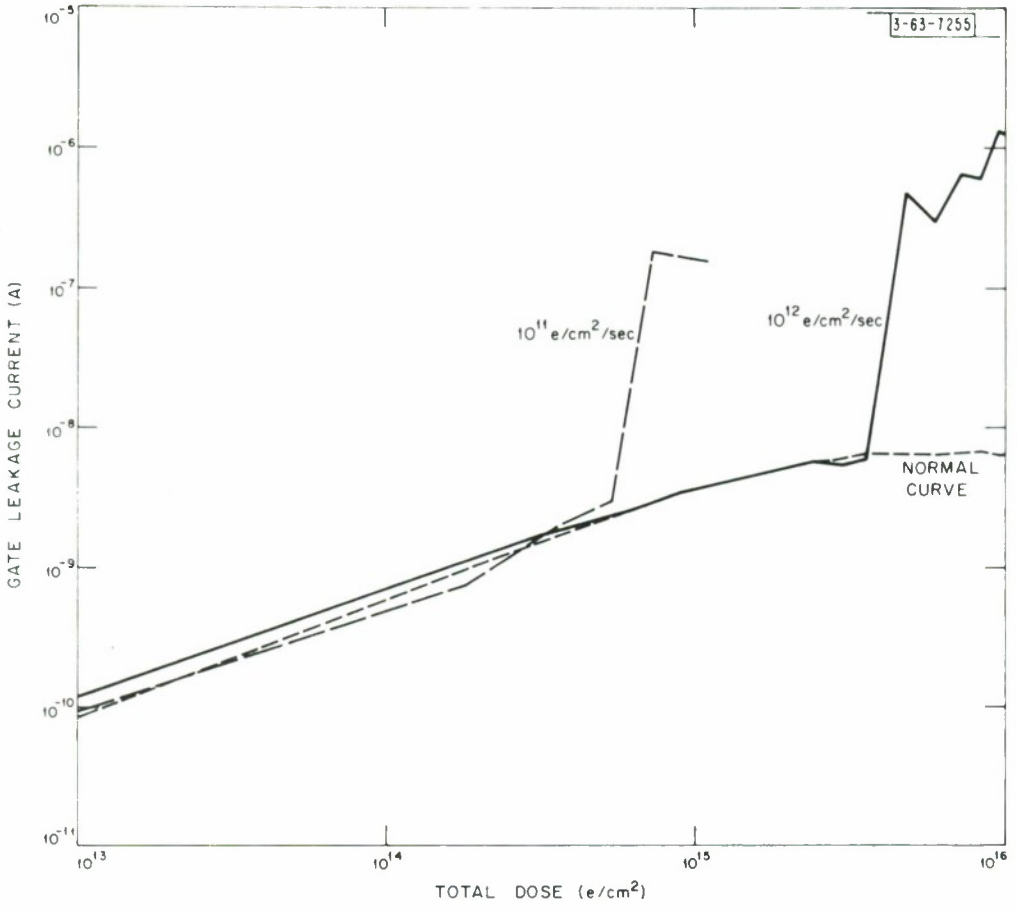

Fig. 7. Anomalous gate leakage current.

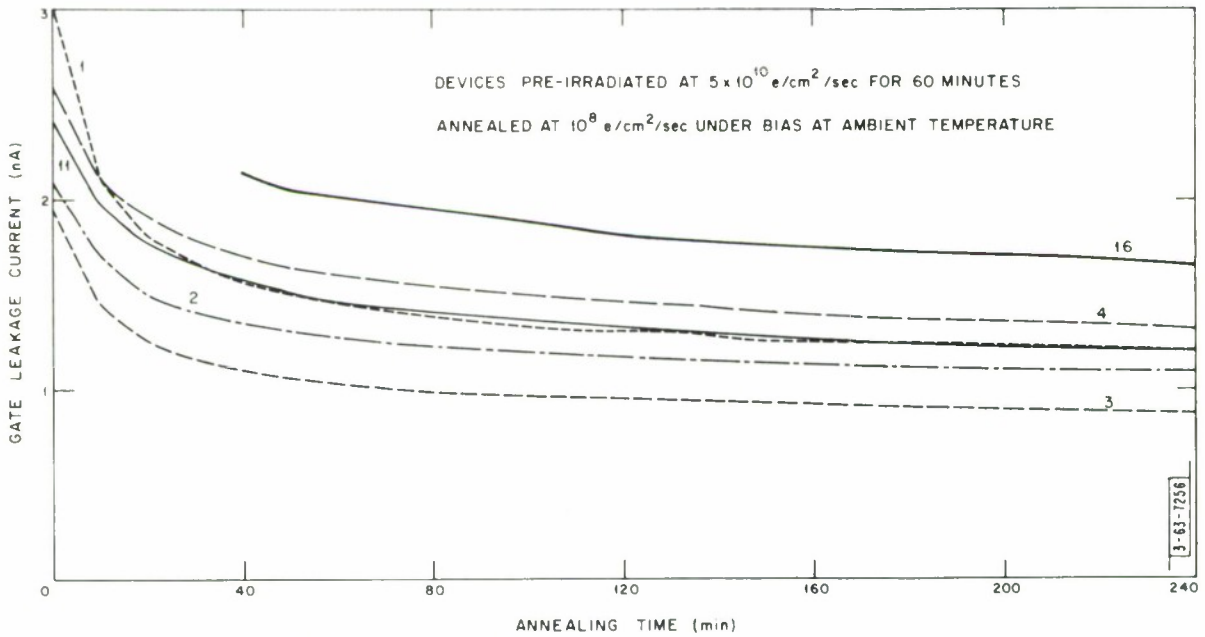

Fig. 8. Real time annealing experiment
Devices preirradiated at 5×10^{10} e/cm^2/sec for 60 minutes, annealed at 10^8 e/cm under bias at ambient temperature

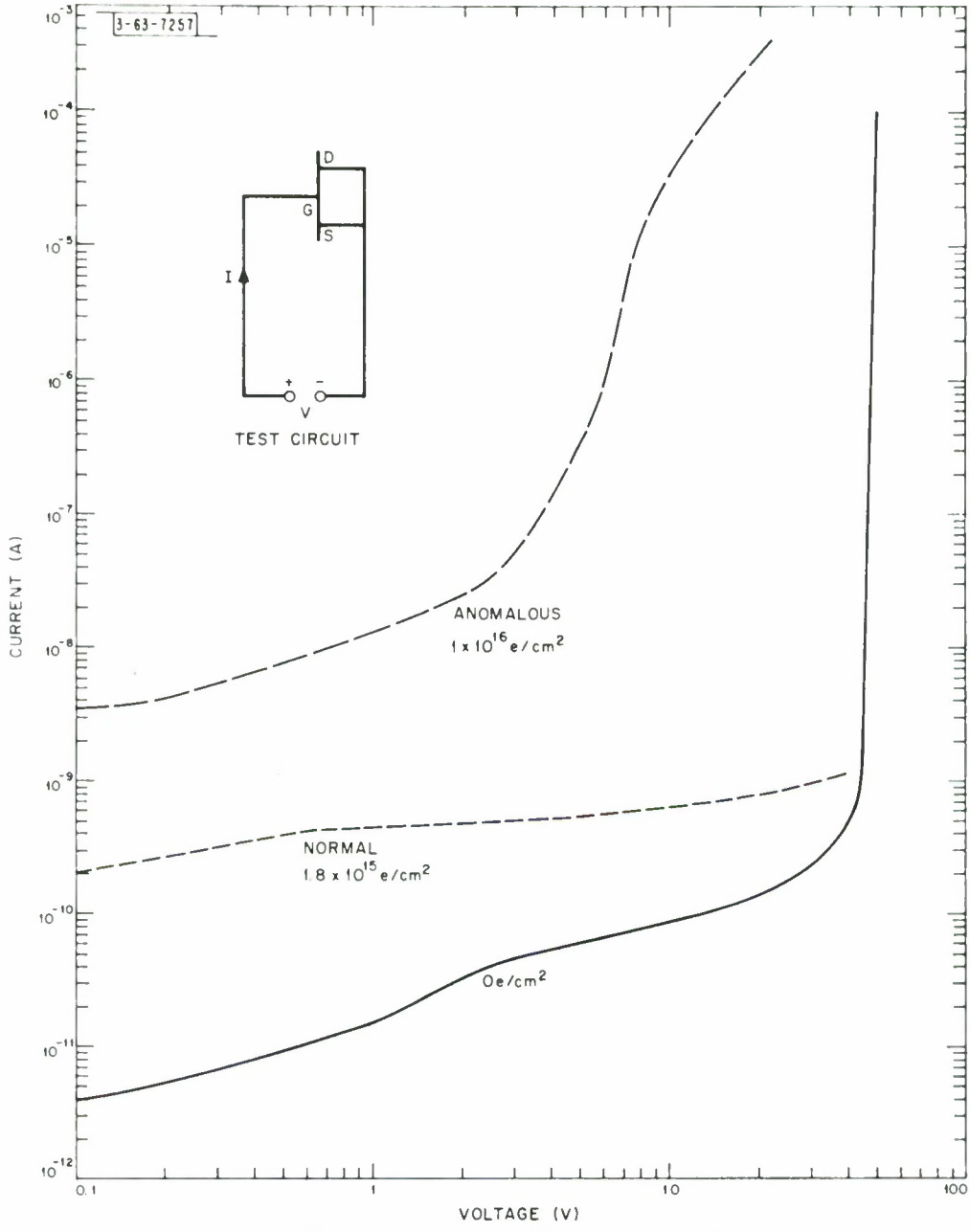

Fig. 9. Reverse I-V characteristics.

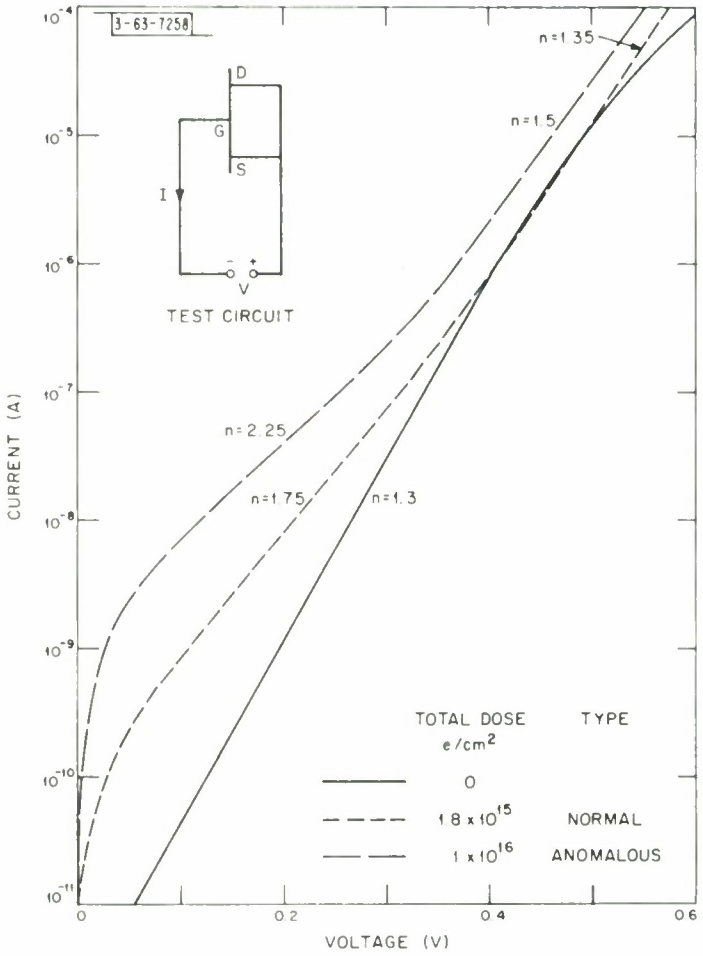

Fig. 10. Forward I-V characteristics.

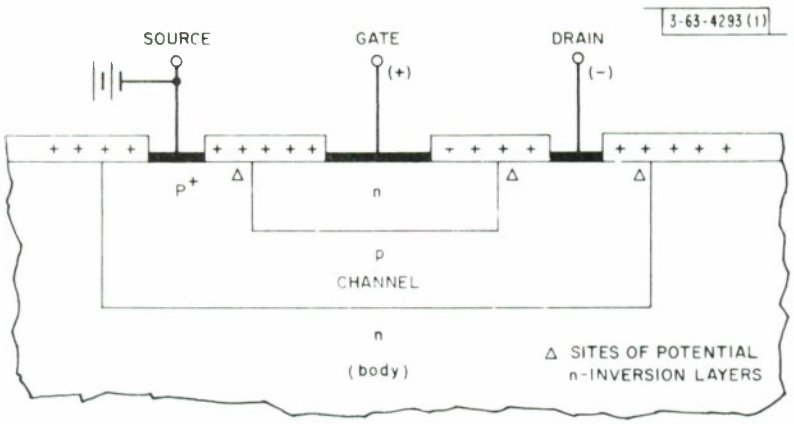

Fig. 11. P-channel FET structure.

REFERENCES

1. A. G. Stanley "Effect of Space Radiation Environment on Micro-Power Circuits Using Bipolar Junction-Gate and Insulated-Gate Field Effect Transistors", NEREM Record, Vol. 8, Nov. 1966, pp. 30-31.

2. A. G. Stanley "Effect of Electron Irradiation on Electronic Devices" Lincoln Laboratory Technical Report 403, 3 November 1965.

3. J. P. Mitchell "Dose Rate Dependence of Surface Radiation Damage Effects in Planar Silicon Devices", NEREM Record, Vol. 8, Nov. 1966, p. 32.

4. C. L. Mack, Jr. "Lincoln Accelerator Laboratory", Lincoln Laboratory Technical Note 1966-12, 2 Sept. 1966.

5. F. S. Goulding "A Survey of the Applications and Limitations of Various Types of Detectors in Radiation Energy Measurement", IEEE Trans. Nucl. Science NS-11, 3, June 1964, pp. 177-190.

6. J. P. Mitchell and D. K. Wilson "Surface Effects of Radiation on Semiconductor Devices", Bell Syst. Tech. J. Vol. 46, 1, Jan. 1967, pp. 1-80.

7. C. A. Goben and F. M. Smits "Anomalous Base Current Component in Neutron Irradiated Transistors", Sandia Corporation Reprint SC-R-64-195, July 1964.

8. C. A. Goben "A Study of the Neutron-Induced Base Current Component in Silicon", IEEE Trans. Nuclear Science, NS-12, No. 5, July 1965, pp. 134-146.

9. G. J. Brucker et al "Ionization and Displacement Damage in Silicon Transistors", IEEE Trans. Nucl. Sci. NS-13, No. 6, Dec. 1966, pp. 188-196.

10. C. T. Sah "Effect of Surface Recombination and Channel on P-N Junction and Transistor Characteristics", IRE Trans. Electron Devices ED-9, 1, Jan. 1962, pp. 94-108.

11. M. A. Xavier "Correlation of Theoretical and Experimental Behavior of Silicon Junction Diodes During Neutron and Gamma Irradiation", Proc. of the Second Conference on Nuclear Radiation Effects on Semiconductor Devices, Materials and Circuits, Sept. 17 and 18, 1959, Cowan Publishing Corp.

12. W. Shockley "The Theory of P-N Junctions in Semiconductors and P-N Junction Transistors", Bell System Tech. J. 28, pp. 435-489, July 1949.

13. C. T. Sah "Effects of Electrons and Holes on the Transition Layer Characteristics of Linearly Graded P-N Junctions", Proc. IRE 49, March 1961, pp. 603-618.

14. C. T. Sah "A New Semiconductor Tetrode, the Surface Potential Controlled Transistor", Proc. IRE 49, Nov. 1961, pp. 1623-1634.

15. A. S. Grove and D. J. Fitzgerald "The Origin of Channel Currents Associated with P^+ Regions in Silicon", IEEE Trans. Electron Devices ED-12, 12, Dec. 1965, pp. 619-626.

16. A. S. Grove and D. J. Fitzgerald "Surface Effects on p-n Junctions: Characteristics of Surface Space-Charge Regions Under Non-Equilibrium Conditions", Solid-State Electronics 9, Aug. 1966, pp. 783-806.

17. V. S. Vavilov "Effects of Radiation on Semiconductors" Consultants Bureau, New York 1965.

18. D. J. Fitzgerald and A. S. Grove "Radiation-Induced Increase in Surface Recombination Velocity of Thermally Oxidized Silicon Structures", Proc. IEEE 54, Nov. 1966, pp. 1601-1602.

DOCUMENT CONTROL DATA – R&D

(Security classification of title, body of abstract and indexing annotation must be entered when the overall report is classified)

1. ORIGINATING ACTIVITY *(Corporate author)* Lincoln Laboratory, M.I.T.	2a. REPORT SECURITY CLASSIFICATION Unclassified 2b. GROUP None

3. REPORT TITLE

Electron Irradiation of P-Channel Junction FETs

4. DESCRIPTIVE NOTES *(Type of report and inclusive dates)*

Technical Note

5. AUTHOR(S) *(Last name, first name, initial)*

Stanley, Alan G.

6. REPORT DATE	7a. TOTAL NO. OF PAGES	7b. NO. OF REFS
13 April 1967	36	18

8a. CONTRACT OR GRANT NO. AF 19(628)-5167 b. PROJECT NO. 649L c. d.	9a. ORIGINATOR'S REPORT NUMBER(S) Technical Note 1967-20 9b. OTHER REPORT NO(S) *(Any other numbers that may be assigned this report)* ESD-TR-67-239

10. AVAILABILITY/LIMITATION NOTICES

Distribution of this document is unlimited.

11. SUPPLEMENTARY NOTES	12. SPONSORING MILITARY ACTIVITY
None	Air Force Systems Command, USAF

13. ABSTRACT

The resistance of p-channel junction FETs to electron irradiation in high impedance nanoamp circuit applications is limited by the leakage current across the gate junction. The dependence of the leakage current on electron flux and total dose was investigated by electron irradiation in vacuum. The increase in leakage current was found to be primarily due to an increase in surface recombination velocity. It was independent of the electron flux over the range from 3×10^9 to 10^{12} e/cm^2/sec with some indication of a reduction in leakage current at lower fluxes. An anomalously high leakage current due to channel formation developed in some devices at total doses above 10^{14} e/cm^2.

14. KEY WORDS

circuits and components
electron irradiation
radiation
semiconductor devices